ISSN: 2414-1895 DOI: 10.6919/ICJE.202412_10(12).0020

Research and Experimental Application of UAV Aeromagnetic Technology in Submarine Pipeline Verification

Bingrou Xi, Shuqiang Li*, Boan Li, Jiajun Xian

Guangdong Marine Development Planning Research Center, Guangzhou, China

*Corresponding Author: Shuqiang Li

Abstract

There are shoals, islands, reefs, aquaculture farms and fishing nets in shallow sea (water depth 0~10m) .With the affected by natural and human factors, it's very difficult to carry out marine survey activities in these shallow sea areas. In order to solve the problem of rapid and efficient pipeline verification in a wide range of shallow sea areas, this paper analyzes the composition and principle of the UAV aeromagnetic survey system, and selects a shallow sea area and coastal zone with submarine pipelines in Guangdong as the test area, and uses the UFO-CS multi-rotor cesium optical pump aeromagnetic measurement system and the MAG-DN20-G4 rotor UAV aeromagnetic detection system to carry out submarine pipeline detection tests in the area between 10 and 30 meters above sea altitude. The magnetic anomalies of the target pipelines at different altitude were compared. The test of UAV aeromagnetic technology in the verification of submarine pipelines in a small area of Guangdong provides a reference for the subsequent verification of submarine pipelines in Guangdong Province and even the whole country, and accumulates experience for exploring efficient magnetic exploration methods for cables in shallow sea areas.

Keywords

UAV; UAV Aeromagnetics; Magnetic Sounding; Submarine Pipeline Verification.

1. Foreword

Since the beginning of the 21st century, unmanned aerial vehicle technology has gradually matured. Due to the technical characteristics of UAV such as small size, light weight, low production cost and suitable for ultra-low-altitude flight, after being equipped with high-precision magnetic measurement equipment as a scientific payload, and then optimized and integrated, the new aeromagnetic measurement system products and their application research have increasingly attracted extensive attention from various aerogeophysical manufacturers or survey institutions in the world.

In recent years, offshore wind power, international optical cable and other marine pipeline projects have developed rapidly, in the process of submarine cable route survey, the pipeline survey in the shallow water area (water depth 0~10m) along the offshore coast has been a difficult problem to solve. The low-altitude and high-precision aeromagnetic measurement technology of UAV has been applied in the land area, and the test effect is good. According to the research of unmanned aeromagnetic technology in China in recent years, it is feasible to carry out low-altitude high-precision aeromagnetic survey of UAV in shallow water area (water depth 0~10m) near coastal water, which can effectively solve the difficulty of buried pipeline investigation in shallow coastal area. In order to solve this difficult problem, the UAV platform and magnetic sensor are combined to detect magnetic targets in the sea-land combination area, and the appropriate flight altitude is selected according to the magnetic characteristics of the target object to obtain low-altitude high-resolution

ISSN: 2414-1895 DOI: 10.6919/ICJE.202412_10(12).0020

space magnetic dataExplore the efficient magnetic exploration method of cable in shallow water area, accumulate experience, further master the key technology of aeromagnetic system, and lay the foundation for the construction of aeromagnetic survey system.

2. Principle and Test Method of UAV Aeromagnetic Measurement System

2.1 Principle

The working principle of aeromagnetic method is a method for magnetic field observation carried by UAVs with magnetic sensor probes. The aeromagnetic measurement system is mainly composed of an aeronautical flight platform, an aeromagnetic instrument, an aeromagnetic compensator, a navigation and positioning system, an altimetry instrument, a diurnal observation system, and a data collation and processing system. The main purpose of using the UAV geomagnetic survey system to detect the nearshore target cable is to distinguish the target cable from the magnetic background field and the interference field, so as to accurately locate the cable direction on the planeCarry out UAV aeromagnetic surveying, UAV obtains the three-component magnetic value of the area by adjusting the flight altitude, encrypting the line of key areas and other means, and then processes the data according to the UAV attitude record and daily change record to eliminate the interference of high-frequency interference of the aircraft body and the short-term change of the geomagnetic field, and obtains the magnetic anomaly distribution characteristics of the area where the cable is located.

On the one hand, the principle of this test is to avoid all equipment that causes interference, such as aircraft engines, servos and aircraft circuit systems, and try to stay away from them. On the other hand, in order to ensure flight safety and conform to the principle of aerodynamics, aerodynamic simulation testing is required. The loading scheme adopted this time is the forward fall loading method, that is, the magnetic sensor is installed in the nose position through an extension rod, which is suitable for the rear engine UAV.

2.2 Instrument and Line Setting

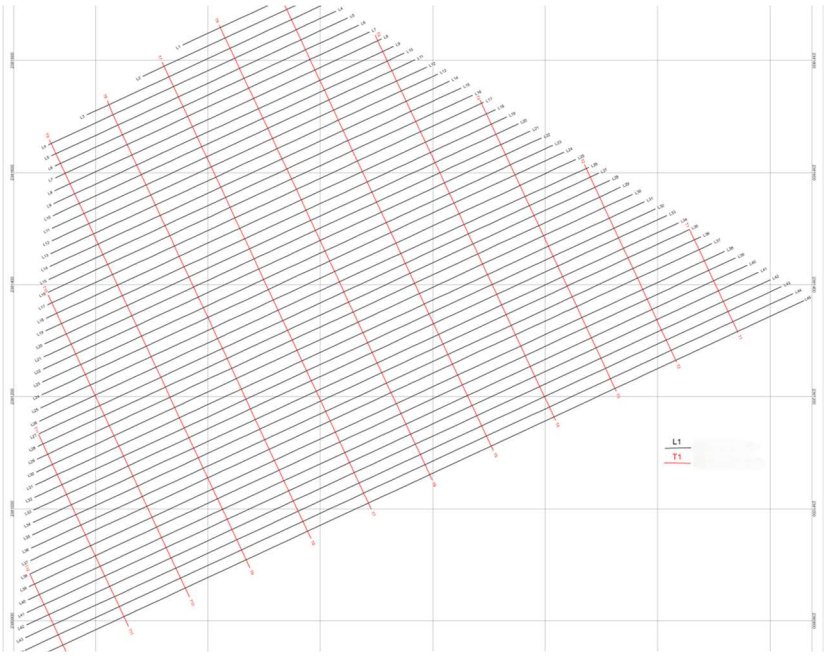

Figure 1. Network diagram of the Y survey area

In this paper, the UFO-CS multi-rotor cesium optical pump aeromagnetic measurement system and the MAG-DN20-G4 rotor UAV aeromagnetic detection system are equipped with high-precision magnetometer and fluxgate sensor of cesium optical pump respectively, and two different measurement element modes are used to complete the aeromagnetic measurement of the pipeline area at an ultra-low altitude of 10m~30m above sea level in the test area.

ISSN: 2414-1895 DOI: 10.6919/ICJE.202412_10(12).0020

The UAV aeromagnetic survey line is laid out on a scale of 1:2000, with a spacing of 20 m and a spacing of 120 m. According to the general data of the submarine pipeline obtained in advance, it is determined that the direction of the survey line in the survey area is 65°, and the direction of the control line is 155°.

2.3 Experimental Testing of UAV Aeromagnetic System

The experimental test of UAV aeromagnetic system includes static noise level test of aeromagnetic instrument, static noise level test of magnetic daily variable base station, aeromagnetic compensation flight, GPS static positioning accuracy test, and consistency testWait.

After the static noise level test of the aeromagnetometer is installed on the UAV and the debugging is completed, the external power supply system is used to power the ground, only the airborne aeromagnetic measurement system is turned on, and the other instruments do not work, and the observation time is not less than 2h. The static noise level is counted at a sampling rate of 2Hz.

For the static noise level test of the magnetic daily variable base station, the magnetic daily variation observation point should be selected in a calm magnetic field, small magnetic gradient, small human interference, and flat and open terrain. And continuous observation for no less than 24 hours, to judge the magnetic interference of the environment, to determine the basis value of magnetic daily variation.

The aeromagnetic compensation flight area is selected in the area where the geomagnetic field is relatively calm and close to the survey area, and the direction of the flight test line should generally be consistent with the direction of the main survey line and the cutting line designed.

Aeromagnetic compensation flight is divided into two flight phases: compensation and post-compensation inspection. After the compensation accuracy obtained in the compensation stage reaches the requirements, another post-compensation inspection flight is carried out. The purpose of the compensation inspection flight is to confirm the effectiveness of the compensation.

GPS static positioning accuracy test, the GPS in the aeromagnetic system needs to observe its static positioning accuracy at a fixed point of the base. It is necessary to continuously observe and record for more than 30 minutes, and calculate the static positioning accuracy according to the observed coordinate data.

Consistency test, when multiple instruments carry out measurement flights at the same time, it is necessary to carry out consistency tests on the ground in advance, and two magnetometers of the same type with equal precision are required to compare and observe, and the measurement difference should be < 0.5nT for 5 consecutive hours.

2.4 Aircraft Magnetic Interference Field Compensation Flight

The magnetic field interference introduced by the UAV platform is the main interference source that limits the advantages of high-precision magnetometers. The interference field of the aircraft is partly due to the electromagnetic interference of the circuit, and partly related to the maneuvering (attitude change) of the aircraft. When the attitude of the aircraft changes, the component of the aircraft interference field in the signal also changes due to the change of the relative position of the aircraft and the geomagnetic field. Generally speaking, magnetic compensation is to study the interference field related to the maneuver of the aircraft in order to eliminate the measured magnetic field signal.

2.4.1 Compensation Model

In this paper, UFO-F is used to compensate aeromagnetic using soft compensation (post-compensation) technology. The compensation model adopts the model of Tolles and Lawson (1944), which divides the aircraft magnetic field related to aircraft maneuvering into residual magnetic field Bp (Permanent field), induced magnetic field Bi (Induced field) and eddy current magnetic field Be (Eddy current field), and the detailed derivation can be referred to the article published by Tolles (1955), which is directly quoted below:

ISSN: 2414-1895 DOI: 10.6919/ICJE.202412_10(12).0020

$$\Delta \mathrm{B} = B_p + B_i + B_e \tag{1}$$

The remaining magnetic field is:

$$\mathrm{B}_p = a_1 \cos X + a_2 \cos Y + a_3 \cos Z \tag{2}$$

a1, a2, a3 are the compensation coefficients of the residual magnetic field, and cosX, cosY, and cosZ are the cosine of the angle between the direction of the geomagnetic field and the three axes of the aircraft.

The induced magnetic field is:

$$\mathrm{B}_i = B\begin{pmatrix} a_4 \cos^2 X + a_5 \cos X \cos Y + a_6 \cos^2 Y + \\ a_7 \cos X \cos Y + a_8 \cos Y \cos Z + a_9 \cos^2 Z \end{pmatrix} \tag{3}$$

a4-a9 is the compensation coefficient of the induced magnetic field, and B is the total geomagnetic field intensity.

The eddy current field is:

$$\mathrm{B}_e = B\begin{bmatrix} a_{10} \cos X(\cos X)' + a_{11} \cos X(\cos Y)' + a_{12} \cos X(\cos Z)' + \\ a_{13} \cos Y(\cos X)' + a_{14} \cos Y(\cos Y)' + a_{15} \cos Y(\cos \mathrm{Z})' + \\ a_{16} \cos Z(\cos X)' + a_{17} \cos Z(\cos Y)' + a_{18} \cos Z(\cos Z)' \end{bmatrix} \tag{4}$$

2.4.2 Compensated Flights

A survey area of about 1 km x 1 km with stable geomagnetic changes, small gradients, and no ground anomalies was selected for compensated flight.

Fly as high as possible to eliminate ground effects.

The daily variation correction of the data of the N group of compensated flights is carried out first, and the vertical gradient correction can also be carried out according to the situation.

List the following equations and solve the (overdetermined) equations:

$$\mathrm{Z}_{(\mathrm{N}*18)} A_{(18)} = \mathrm{B}_{(N)} \tag{5}$$

Z is the coefficient matrix composed of each set of measured attitude data, F is the geomagnetic field value of each measurement point, and A is 9 or 18 undetermined coefficients.

Nonlinear regression methods (least squares, Robust estimation, ridge regression, etc.) were used to obtain a total of 18 undetermined coefficients from a1 to a18.

For example, least squares:

$$Z^T ZA = Z^T B \tag{6}$$

ISSN: 2414-1895 DOI: 10.6919/ICJE.202412_10(12).0020

2.4.3 Compensate for the Measured Flight Data

Compensate for each group of data actually measured, substitute the coefficient composed of attitude data and the a1-a18 undetermined coefficient solved by compensation flight into equation (1)(2)(3)(4) to obtain the aircraft interference field, and subtract the aircraft interference field after the measured magnetic field data is corrected by daily variation, and obtain the compensated magnetic field value:

$$\mathrm{B}_{bc} = B - \Delta B \tag{7}$$

In addition, during the operation of the UAV aeromagnetic system, it is also necessary to observe the ground magnetic diurnal variation and repeat the line flight.

3. Research Results and Analysis of UAV Aeromagnetics

According to the actual measurement results in the test area, the magnetic field information is abundant, and the magnetic anomaly corresponds to the distribution of the submarine pipeline. It shows that the layout of the measuring network is reasonable, and the expected measurement effect is obtained.

3.1 Interpretation of Magnetic Anomalies in Aeromagnetic Data of Cesium Optical Pumps

The aeromagnetic survey of the fluxgate sensor has completed the 30-meter, 20-meter, and 10-meter altitude measurement tasks in the test area, with 135 effective survey lines with a cumulative length of about 137.4km, 36 control lines with a cumulative length of about 84km, 16 control lines with a cumulative length of about 13km, and a measurement area of 1.3km2.

The aeromagnetic measurement of cesium optical pump sensor has completed the 20-meter and 30-meter altitude measurement tasks in the test area, with 90 effective survey lines with a cumulative length of about 165km, and 24 control lines with a cumulative length of about 10km and a measurement area of 1.6km2.

As can be seen from the original plane contours in Figure 2, the anomalies are mainly concentrated in A1 and A2.Recently, the overall distribution of anomalies is high in the southeast and low in the southwest, and the magnetic anomalies are different, including equiaxed, planar and banded, and the amplitude is different. A1 anomalies are abundant, mainly punctate and faceted positive anomalies. A2 is relatively simple, mainly composed of two faceted positive anomalies. The positive and negative boundaries of the A3 anomaly are obvious, because only a small amount of data is collected at the boundary of the flight area, and the direction and shape of the anomaly cannot be judged.

Figure 3 shows the ΔT diagram of the measurement area (ΔT is the measured value minus the background field value), and the maximum value of the measured △T magnetic anomaly is 120 nT and the minimum value is -101 nT. In order to eliminate the accompanying anomalies caused by oblique magnetization, enhance the correspondence between the geomagnetic field and the magnetic anomaly, and make the boundary of the magnetic anomaly clearer, the polarization is treated. Figure 4 shows the plane diagram of the aeromagnetic anomaly after △T polarization (ΔT electrodeterization: input file ΔT file and magnetic inclination angle and magnetic declination angle information to obtain the polarization results), after polarization, the anomaly distribution mainly changes to a strip distribution, the anomaly in the southeast survey area decreases, and the anomaly in the middle and southwest corners is enhanced. The contour plots of the plane behind the ΔT and ΔT poles are quite different, indicating that the shallow anomaly in this work area is more prominent.

Compared with Figures 3 and 4, the maximum value of the anomaly becomes 223 nT and the minimum value becomes -83 nT, and the amplitude of the positive anomaly changes greatly, while the amplitude of the negative anomaly increases relatively small, indicating that the positive magnetic anomaly in the whole region is more prominent, and the local anomaly is more obvious after polarization.

ISSN: 2414-1895 DOI: 10.6919/ICJE.202412_10(12).0020

In order to understand the characteristics of the local magnetic field, the methods of downward extension, multi-derivative and wavelet transform are used. Figure 5 is the anomaly plane diagram of the downward extension of 5m, due to the high measurement accuracy, the point distance is small, and the oscillation begins to occur after the extension to 10 point distances, compared with the anomalies in Figure 3, it can be seen that the extension makes the amplitude of the local anomaly larger, which plays the role of highlighting the shallow anomaly, but because the point distance is too small, the extension distance is limited, and the anomaly does not change much in general.

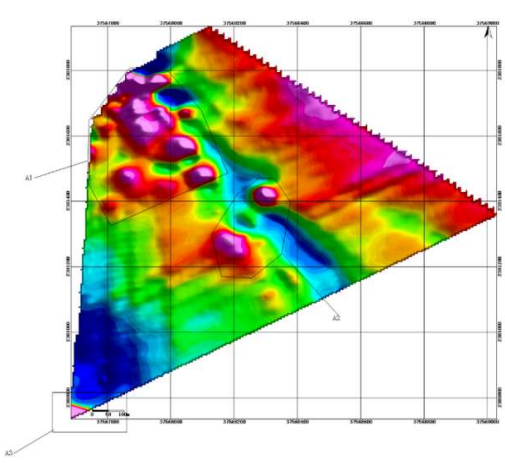

Figure 2. Original plane contour diagram

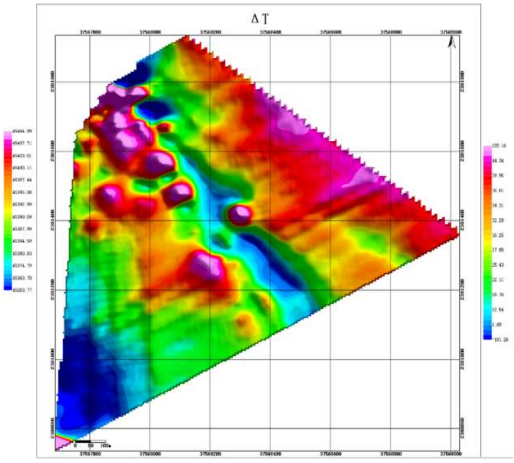

Figure 3. ΔT plane contour diagram

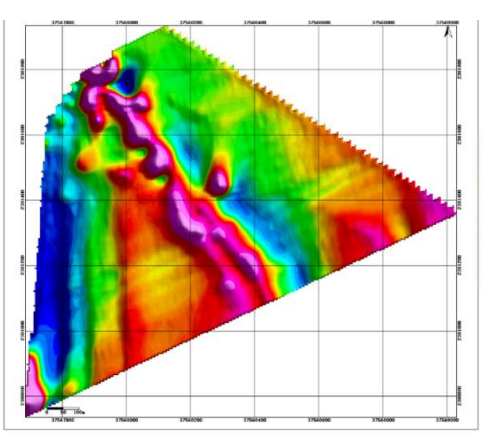

Figure 4. ΔT polarized plane contour plot

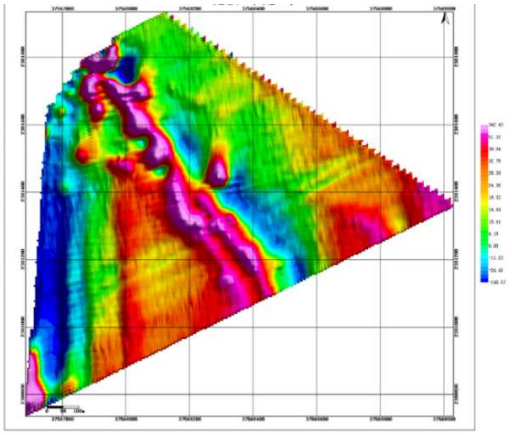

Figure 5. Plane contour plot of 5m extension of ΔT

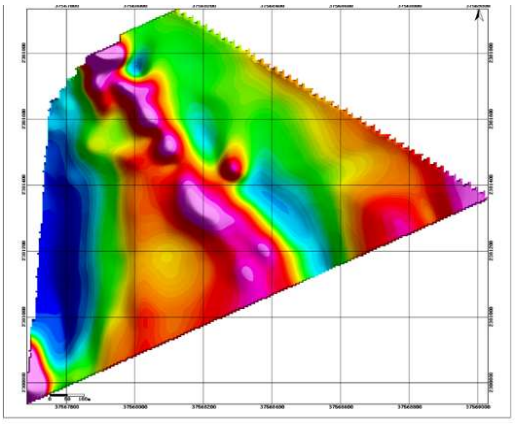

Figure 6. Plane contour plot of 20m extension of ΔT

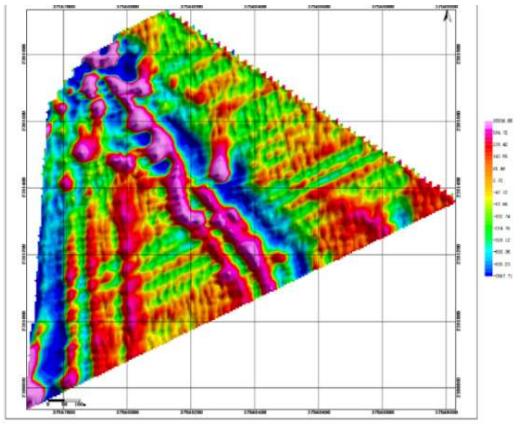

Figure 7. The vertical first-order conductor

ISSN: 2414-1895 DOI: 10.6919/ICJE.202412_10(12).0020

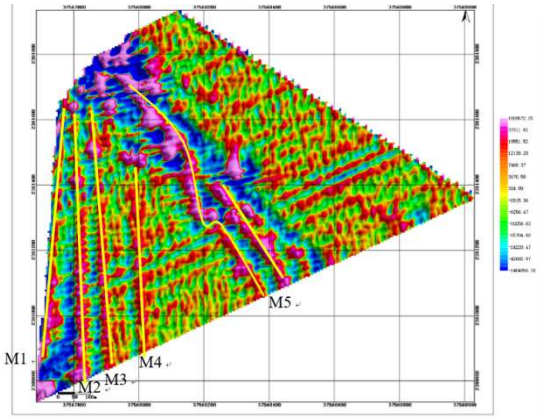

Figure 8. Vertical second-order guide

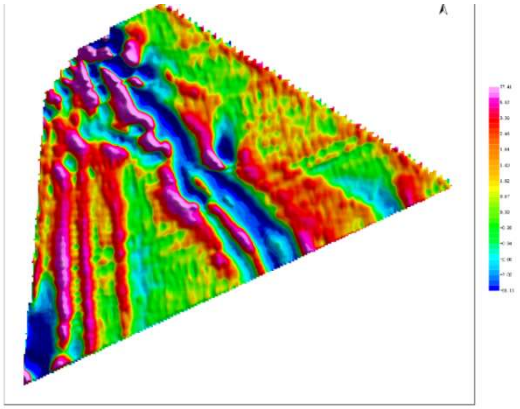

Figure 9. Detail of wavelet decomposition

Figure 8 shows the aeromagnetic vertical second derivative anomaly, highlighting the local anomaly, from which it can be seen that the anomaly is mainly divided into five bar anomalies, named M1-M5 from west to east, among which the M2-M4 anomaly is stronger, the anomaly connection is obvious, and the trend is clear. M1 is relatively weak because it is at the boundary of the work area, but it also has a certain continuity, and its authenticity needs to be verified. The anomaly of M5 is the most prominent in the whole map, its anomalous morphology is more tortuous than that of M2-M5, the anomalous continuity is relatively poor, and M5 is bifurcated in the southern region, and the anomaly trend is similar to that of M5. There is a slight associated linear magnetic anomaly on the east side of M3, which may be a smaller magnetic anomaly. The specific anomalies of M1-M5 are subject to later field investigation and verification.

Compared with other diagrams, the most significant change in the vertical second-order guide plane contour map is the appearance of a relatively obvious anomaly M1 at the western boundary, and the magnitude of the amplitude reflects the scale and magnetic content. The details of wavelet variation 1 are close to the results of the vertical second derivative, and the location of the shallow high magnetic anomaly mainly refers to the second derivative anomaly, while the deep high magnetic anomaly refers to the extension anomaly, which depends on the research objectives.

3.2 Magnetic Anomaly Interpretation of Fluxgate Aeromagnetic Data

3.2.1 Local Anomalies of Aeromagnetic ΔT in the Test Area

When the relative sea surface altitude is about 20 meters, the obvious band-like and bead-like anomalies are identified according to the local anomalous distribution characteristics of ΔT. A total of 11 submarine pipelines are inferred, numbered TL1, TL2, TL3, TL4, TL5, TL6, TL7, TL8, TL9, TL10, and TL11 (Figure 10).

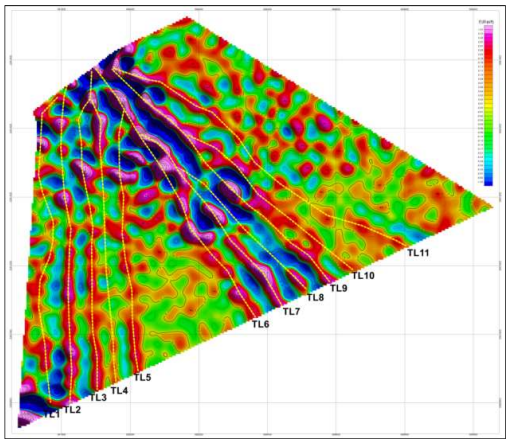

Figure 10. Inferred diagram of aeromagnetic anomaly

ISSN: 2414-1895 DOI: 10.6919/ICJE.202412_10(12).0020

When the relative sea surface altitude is about 30 meters, the obvious banded and beaded anomalies are identified according to the local anomaly distribution characteristics of ΔT. A total of 10 submarine pipelines were inferred, numbered TL1, TL2, TL3, TL4, TL5, TL6, TL7, TL9, TL10, and TL11 (Figs. 11), which corresponded to the large-scale survey area, but lacked the identification of TL8 anomalies and the continuity of the anomalies was poor.

When the altitude is about 10 meters relative to the sea surface, the obvious banded and beaded anomalies are identified according to the local anomaly distribution characteristics of ΔT. A total of 11 submarine pipelines were inferred, numbered TL1, TL2, TL3, TL4, TL5, TL6, TL7, TL8, TL9, TL10, and TL11 (Fig. 12), with obvious abnormal linearity and good continuity.

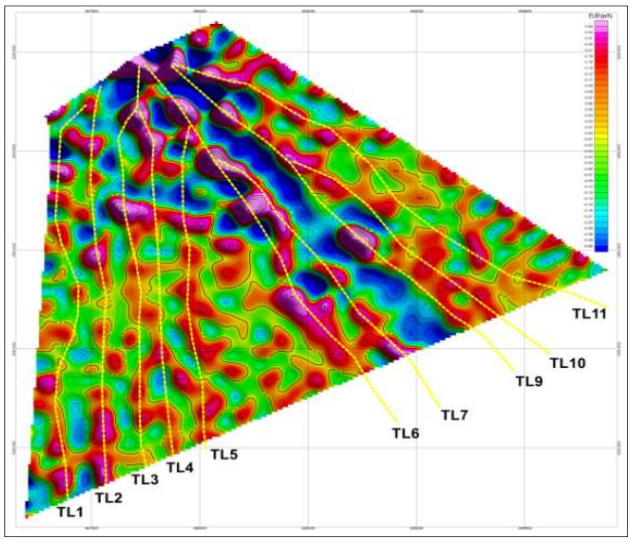

Figure 11. Inferred diagram of aeromagnetic anomaly(altitude 30m)

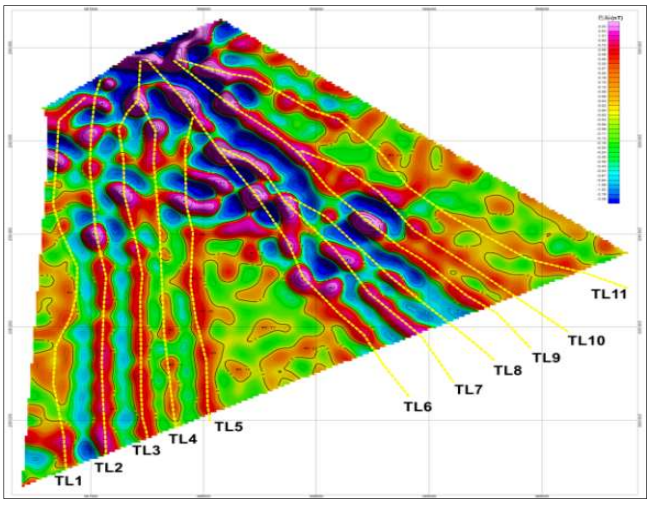

Figure 12. Inference diagram of aeromagnetic anomaly(altitude of 10m)

4. Conclusion

By using the aeromagnetic systems of two different magnetic sensors, cesium optical pump and fluxgate, the aeromagnetic survey of the submarine pipelines in the Y and Z test areas is carried out, and the buried and exposed submarine cables and communication optical cables in the intertidal zone to the water depth of 1 0 m can be detected by the two aeromagnetic systems, and the plane position information of the submarine pipelines can be obtained through interpretation.

ISSN: 2414-1895 DOI: 10.6919/ICJE.202412_10(12).0020

According to the figure, it can be seen that with the increase of the altitude of the UAV aeromagnetic system, the magnetic anomaly of the pipeline target gradually weakens, and the lower the aeromagnetic height, the more obvious the magnetic anomaly of the pipeline target. According to the collected data, 12 submarine cables in the test area have been logged in a centralized manner, and 11 can be interpreted by the aerial data of the fluxgate sensor.

Due to the special installation of the magnetic probe of the cesium optical pump, the flight height of 10m is a flight safety hazard, so the field has completed the magnetic measurement of the cesium optical pump sensor with two flight heights of 20m-30m in the test area, and the magnetic anomaly intensity of the 20m and 30m altitude is almost the same compared with the fluxgate sensor. The data of the 20m altitude of the cesium optical pump aeromagnetic system can be interpreted 9 pieces.

Acknowledgments

Fund project:

1) Verification of offshore submarine pipelines in Guangdong Province

2) Research on key technologies for integrated observation of marine environment “Space-Air-Ground-Sea Integrated Network”based on the National Comprehensive Marine Experimental Ground (Zhuhai)

References

[1] Yang YK. Research on rapidde tection technology of dronesin complex environments [D].Beijing:China University of Geosciences,2020.

[2] Zhang J,Bao SC,Peng X K.New method of green exploration:Low altitude aeromagnetic survey[J].Gansu Geology,2018,27(2):78-82.

[3] Li Zhipeng, Gao Song, Wang Xuben. 2018. New method of aeromagnetic surveys with rotorcraft UAV in particular areas[J]. Chinese Journal of Geophysics,61(9):3825-3834.

[4] Liu Shuang, Hu Xiangyun, Guo Ning, C ai Hongzhu, Zhang Henglei,Li Yongtao. 2023. Overview on UAV aeromagnetic survey technology[J]. Geomatics and Information Science of Wuhan University,48(6): 823-840.

[5] Qiao Zhongkun, Ma Guoqing, Zhou Wenna, Yu Ping, Zhou Shuai, Wang Taihan, Tang Shuiliang, Dai Weiming, Meng Zhaohai, Zhang Zhihou. 2020. Research on aeromagnetic compensation of a multirotor UAV based on robust principal component analysis[J]. Journal of Applied Geophysics,63(12):4604-4612.

[6] Zhou Puzhi, Li Zhengyuan, Tang Minqiang, Tang Shuiliang, Wang Fei, Yang Jia. 2023. Application test of aeromagnetic technology of ultra-low altitude UAV in submarine cable detection[J].Hydrographic Surveying and Charting,43(4): 10-14.

[7] Ma Guoqing,Zhang Yun,Guo Jingxue,Li Lili, Jiang Zhexin, Gao Tong.2023. First application test of aeromagnetic system of rotorcraft UAV in princess elizabeth land of southeast Polar region[J]. Progress in Geophysics,38(1):484-493.

[8] Yue Xiangping,Guo Wenbo,Chen Zonggang,et al.Research and application of low altitude aeromagnetic method under complex conditions[J].Chinese Journal of Engineering Geophysics,2024,21(3):383-392.

[9] CAI Xuan, XU Baohua, LI Daopeng et al., Integrated submarine cable detection methods and applications[J]. EXPRESS WATER RESOURCES & HYDROPOWER INFORMATION, 2023,44(10): 36-40.